

# Catalyst Morphology and Dissolution Kinetics of Self-Healing Polymers

Alan S. Jones,<sup>\*,†</sup> Joseph D. Rule,<sup>‡</sup> Jeffrey S. Moore,<sup>‡</sup> Scott R. White,<sup>§</sup> and Nancy R. Sottos<sup>†</sup>

*Theoretical and Applied Mechanics Department, Department of Chemistry, and Department of Aerospace Engineering, University of Illinois, Urbana, Illinois 61801*

*Received August 18, 2005. Revised Manuscript Received January 3, 2006*

The role of the crystal morphology and dissolution kinetics of Grubbs' catalyst on self-healing capability is examined. Self-healing polymers require complete coverage of the crack plane with polymerized healing agent for optimal recovery of mechanical integrity. Lack of catalyst leads to incomplete coverage, partial polymerization, and poor mechanical recovery. Catalyst availability is determined by the competing rates of dissolution of the catalyst and polymerization of the healing agent. First-generation Grubbs' catalyst exists in at least two crystal polymorphs, each with a distinct crystal shape, thermal stability, and dissolution kinetics. The more rapidly dissolving polymorph shows superior healing efficiency when used as the initiator in a self-healing epoxy material based on ring-opening metathesis polymerization of dicyclopentadiene.

## Introduction

Self-healing polymer composites consist of encapsulated healing agent and catalyst particles embedded in a polymer matrix. As a crack propagates through the matrix it ruptures the microcapsules, releasing the healing agent into the crack plane through capillary action.<sup>1</sup> The current study uses a self-healing system with EPON 828/DETA epoxy as the matrix and dicyclopentadiene (DCPD) as the healing agent along with bis(tricyclohexylphosphine)benzylideneruthenium(IV) dichloride (Grubbs' catalyst).<sup>2</sup> Poly(dicyclopentadiene) (pDCPD) is formed by ring-opening metathesis polymerization<sup>3,4</sup> (ROMP) after the monomer comes in contact with an exposed catalyst particle. The newly formed pDCPD layer bonds the crack plane closed and effectively heals the fractured polymer.

The recovery of mechanical properties after a fracture event depends on the interplay between the mechanical and chemical kinetics of the system. In the case of unstable crack growth, where the polymer composite is quickly fractured and mechanical kinetics are rapid, the chemical kinetics determine the extent to which polymerization can occur for a given time and temperature. Brown et al.<sup>5</sup> determined the amount of time required for recovery of the mechanical toughness of the polymer by performing fracture tests on

healed specimens at intervals ranging from 10 min to 72 h after the initial fracture event. No measurable recovery of mechanical properties occurred until approximately 25 min, which closely corresponds to the gelation time of the pDCPD at room temperature at a catalyst concentration of 2 g/L. The recovery of mechanical properties reached steady-state values within 10 h after the initial crack event.

During crack growth under fatigue (cyclic) loading the competition between the mechanical kinetics of crack propagation and the chemical kinetics of polymerization dictates the ultimate performance of a self-healing polymer. A slowly growing fatigue crack can be completely arrested during the loading process, while a fast growing fatigue crack may require rest periods to achieve significant life extension.<sup>6</sup>

Kessler et al.<sup>4</sup> investigated the chemical kinetics of the DCPD/Grubbs' healing system and showed that the degree of cure depends strongly on the catalyst concentration and healing temperature. Kessler's experiments were performed on homogeneous samples with known amounts of Grubbs' catalyst dissolved in DCPD. For self-healing polymers the effective concentration of catalyst will depend on the availability of exposed catalyst on the fracture plane as well as the rate of dissolution of the catalyst in the DCPD. Even with large amounts of catalyst exposed on the fracture plane, the effective concentration of Grubbs' catalyst in the DCPD healing agent may be relatively low if the rate of dissolution of the catalyst is slow.

In this paper we show that Grubbs' catalyst can exist in at least two different crystal morphologies. We also show that the morphology and dimensions of the individual crystals have an important effect on the dissolution kinetics and the healing performance.

\* To whom correspondence should be addressed. Phone: (317) 274-9717. Fax: (317) 274-9744. E-mail: alsjones@iupui.edu.

<sup>†</sup> Theoretical and Applied Mechanics Department.

<sup>‡</sup> Department of Chemistry.

<sup>§</sup> Department of Aerospace Engineering.

(1) White, S.; Sottos, N.; Geubelle, P.; Moore, J.; Kessler, M.; Sriram, S.; Brown, E.; Viswanathan, S. *Nature* **2001**, *409*, 794–797.

(2) Schwab, P.; Grubbs, R.; Ziller, J. *J. Am. Chem. Soc.* **1996**, *118*, 100–110.

(3) Wu, Z.; Benedicto, A.; Grubbs, R. *Macromolecules* **1993**, *26*, 4975–4977.

(4) Kessler, M.; White, S. *J. Polym. Sci., Part A: Polym. Chem.* **2002**, *40*, 2373–2383.

(5) Brown, E.; Sottos, N.; White, S. *Exp. Mech.* **2002**, *42*, 372–379.

(6) Brown, E.; White, S.; Sottos, N. *Compos. Sci. Technol.* **2005**, *65*, 2474–2480.

## Experimental Section

All reagents were used as received from Sigma-Aldrich unless otherwise specified. Decahydronaphthalene (decalin) was dried over molecular sieves in an Ar-filled glovebox.  $\text{CH}_2\text{Cl}_2$  and benzene were vacuum distilled over  $\text{CaH}_2$  under  $\text{N}_2$ . NMR spectra were obtained using a Varian Unity 500 instrument in  $\text{CD}_2\text{Cl}_2$ . ESEM images were taken with a Philips XL30 ESEM-FEG instrument using samples that had been sputter coated with gold–palladium. DSC was performed in aluminum crucibles with a Mettler Toledo DSC821<sup>e</sup> instrument and a heating rate of 1 °C/min. X-ray powder diffraction measurements were performed with a Bruker P4RA X-ray diffractometer using GADDS and a  $\text{Cu K}\alpha$  rotating anode equipped with a graphite monochromator. The beam width at the sample was approximately 0.6 mm. The powder sample was placed in a glass tube with very thin walls (<0.1 mm). The scattering image of the empty tube was subtracted from the data.

**Data for Grubbs' Catalyst from Strem.**  $^1\text{H}$  NMR (500 MHz,  $\text{CD}_2\text{Cl}_2$ ,  $\delta$ ): 20.01 (s, 1H), 8.45 (d,  $J = 7.7$  Hz, 2H), 7.56 (dd,  $J = 7.6$  Hz, 1H), 7.33 (dd,  $J = 7.4$  Hz, 2H), 2.61 (m, 6H), 1.72 (m, 30H), 1.42 (m, 12H), 1.20 (m, 18H). Anal. Calcd for  $\text{C}_{43}\text{H}_{72}\text{Cl}_2\text{P}_2\text{Ru}$ : C, 62.76; H, 8.82; Cl, 8.62; P, 7.53; Ru, 12.28. Found: C, 62.31; H, 9.26; Cl, 9.32; P, 7.83; Ru, 11.78.

**Data for Grubbs' Catalyst from Sigma-Aldrich.**  $^1\text{H}$  NMR (500 MHz,  $\text{CD}_2\text{Cl}_2$ ,  $\delta$ ): 20.01 (s, 1H), 8.44 (d,  $J = 7.4$  Hz, 2H), 7.55 (dd,  $J = 7.3$  Hz, 1H), 7.33 (dd,  $J = 7.7$  Hz, 2H), 2.61 (m, 6H), 1.72 (m, 30H), 1.42 (m, 12H), 1.20 (m, 18H). Anal. Calcd for  $\text{C}_{43}\text{H}_{72}\text{Cl}_2\text{P}_2\text{Ru}$ : C, 62.76; H, 8.82; Cl, 8.62; P, 7.53; Ru, 12.28. Found: C, 62.68; H, 8.93; Cl, 8.74; P, 8.62; Ru, 12.13.

**Recrystallization of Grubbs' Catalyst.** Recrystallization by solvent evaporation was achieved by dissolving Sigma-Aldrich Grubbs' catalyst (0.25 g) in  $\text{CH}_2\text{Cl}_2$  (3 mL) followed by exposure to vacuum at room temperature. For recrystallization by addition of a nonsolvent, Sigma-Aldrich catalyst (0.25 g) was again dissolved in  $\text{CH}_2\text{Cl}_2$  (3 mL). The solution was cooled to  $-20$  °C in an ethylene glycol/ethanol bath<sup>7</sup> and held at that temperature for 5 min. Subsequently, cold acetone (1.5 mL,  $\sim 0$  °C) was added to the solution at a rate of 0.1 mL/min, during which time a precipitate formed. These crystals were collected by filtration and placed under vacuum to dry. For freeze-drying, Sigma-Aldrich Grubbs' catalyst (0.50 g) was dissolved in benzene (10 mL) and the solution was frozen in a liquid nitrogen bath. The sample was then placed on a freeze-drier at  $-83$  °C and 17 mTorr, and the benzene was allowed to sublime for 24 h.

**Dissolution Kinetics.** The dissolution kinetics measurements were performed by placing four samples of 30 mg of each catalyst in separate vials together with 10 mL of decalin. After specified times each solution was vacuum filtered, and the concentration of Grubbs' catalyst in the solution was measured by ultraviolet/visible absorbance on a Shimadzu UV-2410PC spectrophotometer. The molar absorptivity for Grubbs' catalyst in decalin at  $\lambda = 528$  nm was measured to be  $\epsilon = 451 \text{ M}^{-1} \text{ cm}^{-1}$ .

**Fracture Testing.** In a typical fracture test, a tapered double-cantilever beam specimen was completely fractured under mode I loading in displacement control, using pin loading and a  $5 \mu\text{m s}^{-1}$  displacement rate. After fracture, the separate halves of the self-healing polymer composite were aligned, and metal clips were placed on the ends of the specimen to hold the halves together. The metal clips did not provide clamping pressure on the fracture planes, but were only used to keep the fracture surfaces of the specimen in contact. The specimen was then allowed to rest at room temperature for 24 h. The clips were removed, and the sample was fractured a second time under mode I loading to measure the

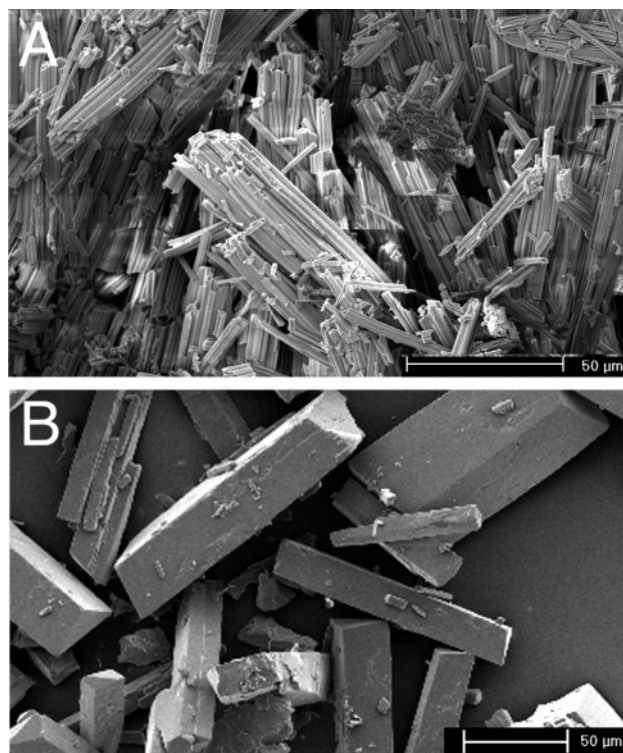


**Figure 1.** ESEM image of (A) Strem Grubbs' catalyst and (B) Sigma-Aldrich Grubbs' catalyst.

healed fracture toughness. Additional details on this method of the fracture testing of self-healing polymer composites can be found in ref 5.

## Results and Discussion

Grubbs' catalyst in the as-received condition was analyzed with NMR, elemental analysis, SEM, DSC, and X-ray powder diffraction. The NMR and elemental analysis confirmed that both catalysts were relatively pure, and the data can be seen in the Experimental Section. Figures 1 and 2 summarize the as-received properties for each type of catalyst. Sigma-Aldrich Grubbs' catalyst is composed of large crystals roughly  $150 \mu\text{m}$  long and  $40 \times 50 \mu\text{m}$  in cross-section (Figure 1B). In contrast, Strem Chemicals Grubbs' catalyst is in the form of crystalline rods about  $100 \mu\text{m}$  in length and only  $2 \mu\text{m}$  in diameter, which are partially fused together in clumps (Figure 1A). X-ray powder diffraction data in Figure 2 indicate that the catalyst samples received from the two suppliers are different crystal polymorphs. Hence, the difference in the crystals is not limited to their dimensions, but the molecules are also arranged in fundamentally different ways.

The crystal polymorph influences the catalyst's thermal stability. DSC traces of the crystals under both nitrogen and air, shown in Figure 3, indicate that the Sigma-Aldrich catalyst remains unaffected at higher temperatures than the Strem catalyst. ROMP trials after thermal exposure show that Sigma-Aldrich catalyst remains active after heating under nitrogen to 190 °C, and the Strem catalyst loses reactivity after 180 °C. Under air, the Sigma-Aldrich catalyst retains its reactivity up to 140 °C while the Strem catalyst begins to decompose at 90 °C. Therefore, the maximum temperature to which a self-healing material can be exposed without being

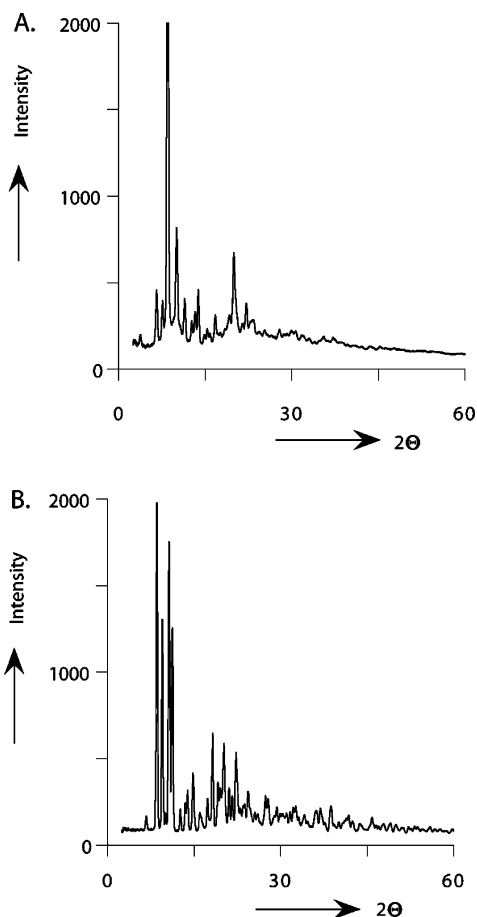


**Figure 2.** X-ray powder diffraction spectra of (A) Strem Grubbs' catalyst and (B) Sigma-Aldrich Grubbs' catalyst.

deactivated is likely to depend on the crystal polymorph that is used.

The morphology of Grubbs' catalyst also has a significant effect on the dissolution kinetics of the DCPD/Grubbs' catalyst system. In general, the smaller crystals provide fast dissolution kinetics. Since August 2003, Grubbs' catalyst is commercially available only through Sigma-Aldrich and in the large crystal form. Two strategies for obtaining smaller catalyst crystal dimensions are presented here. The first involves grinding the as-received catalyst into smaller crystals, while the second requires recrystallizing the catalyst to obtain other morphologies.

In the first case, Grubbs' catalyst was ground with a mortar and pestle for 30 min under an argon atmosphere. Many of the larger crystals were broken into smaller crystals, and some of the catalyst was reduced to submicrometer particles that cover the surface of the larger crystals.

As an alternative to grinding, Grubbs' catalyst was also recrystallized. Depending on the method of recrystallization, different catalyst morphologies are produced. Figure 4 summarizes the results of three different methods of recrystallizing Grubbs' catalyst. Recrystallization by solvent evaporation (Figure 4A) produced catalyst with a morphology similar to that of the original Sigma-Aldrich Grubbs' catalyst, but with slightly smaller dimensions, approximately 75  $\mu\text{m}$  long and 20  $\times$  15  $\mu\text{m}$  in cross-section. As expected, the X-ray powder diffraction data (Figure 5A) for this sample appear

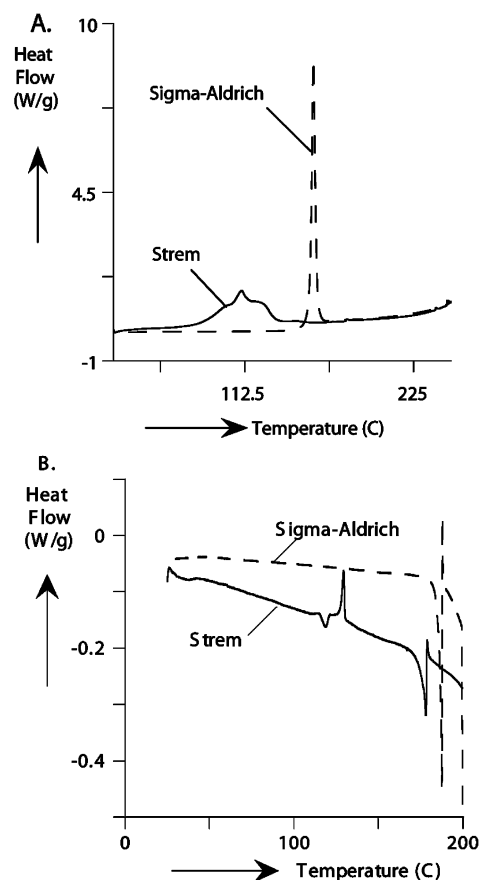


**Figure 3.** DSC traces of Strem and Sigma-Aldrich Grubbs' catalyst at 1  $^{\circ}\text{C}/\text{min}$  (A) under air and (B) under nitrogen.

similar to those for the original Sigma-Aldrich Grubbs' catalyst.

Figure 4B is an ESEM image of Grubbs' catalyst that has been recrystallized by the addition of acetone. The resulting catalyst exhibits a rodlike morphology and X-ray powder diffraction data (Figure 5B) that are similar to those of the original Strem Chemicals sample. A completely different morphology (Figure 4C) was obtained by a recrystallization procedure based on freeze-drying. The resulting morphology is disklike platelets roughly 30  $\mu\text{m}$  in diameter and 1  $\mu\text{m}$  thick. The X-ray powder diffraction data (Figure 5C) show a combination of both crystal polymorphs.

Dissolution studies are commonly used for geochemistry,<sup>8–15</sup> thin film,<sup>16,17</sup> and polymer<sup>18–25</sup> applications and employ many

- (8) Luttge, A.; Bolton, E.; Lasaga, A. *Am. J. Sci.* **1999**, *299*, 652–678.
- (9) Zhang, H.; Bloom, P. *Soil Sci. Soc. Am. J.* **1999**, *63*, 815–822.
- (10) Tunc, M.; Yapici, S.; Kocakerim, M.; Yartasi, A. *Chem. Biochem. Eng. Q.* **2001**, *15* (4), 175–180.
- (11) Zaihua, L.; Wolfgang, D. *Sci. China, Ser. B* **2001**, *44* (5), 500–509.
- (12) Higgins, S.; Jordan, G.; Eggleston, C. *Geochim. Cosmochim. Acta* **2002**, *66* (18), 3201–3210.
- (13) Cheah, S.; Kraemer, S.; Cervini-Silva, J.; Sposito, G. *Chem. Geol.* **2003**, *198*, 63–75.
- (14) Ekmekyapar, A.; Oya, R.; Kunkul, A. *Chem. Biochem. Eng. Q.* **2003**, *17* (4), 261–266.
- (15) Arvidson, R.; Beig, M.; Luttge, A. *Am. Mineral.* **2004**, *89*, 51–56.
- (16) Cooper, W.; Krasicky, P.; Rodriguez, F. *J. Appl. Polym. Sci.* **1986**, *31*, 65–73.
- (17) Manjkow, J.; Papanu, J.; Soong, D.; Hess, D.; Bell, A. *J. Appl. Phys.* **1987**, *62* (2), 682–688.
- (18) Reed, C.; Li, X.; Reed, W. *Biopolymers* **1989**, *28*, 1981–2000.
- (19) Ghosh, S.; Kobal, I.; Zanette, D.; Reed, W. *Macromolecules* **1993**, *26*, 4685–4693.

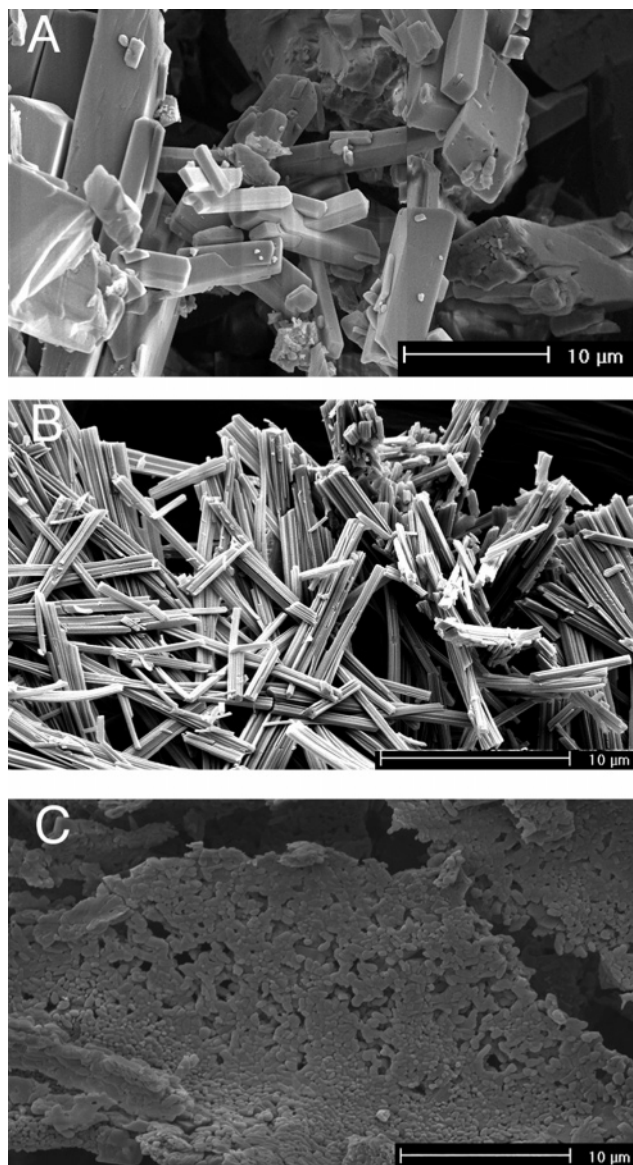


**Figure 4.** ESEM images of Grubbs' catalyst after recrystallization by (A) vacuum evaporation from  $\text{CH}_2\text{Cl}_2$ , (B) precipitation from  $\text{CH}_2\text{Cl}_2$ /acetone, and (C) freeze-drying from benzene.

diverse techniques. Here, the dissolution kinetics of various types of Grubbs' catalyst were investigated by measuring the concentration of the catalyst in decalin through UV spectroscopy after varying dissolution times. Decalin was chosen as a solvent due to its solvating ability toward Grubbs' catalyst, which is likely to be similar to that of DCPD (healing agent) while not being complicated by DCPD's reactivity to the catalyst.

Figure 6 presents the dissolution rates of the catalysts. The large crystal (Sigma-Aldrich) Grubbs' catalyst has a relatively slow dissolution rate and is only 27% dissolved after 37.5

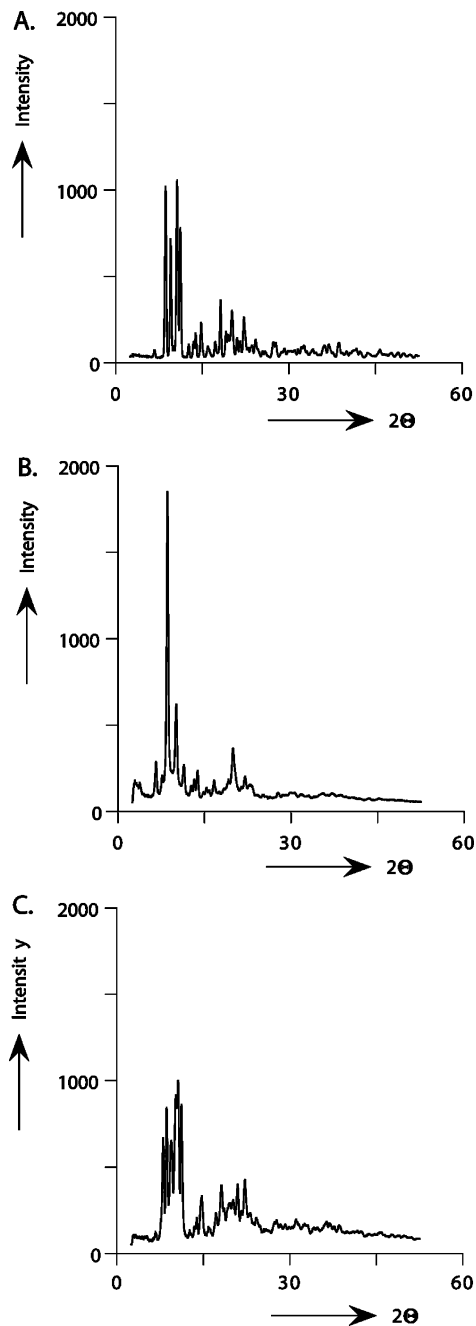


**Figure 5.** X-ray powder diffraction profiles of Sigma-Aldrich Grubbs' catalyst after recrystallization by (A) vacuum evaporation, (B) precipitation in acetone, and (C) freeze-drying.

min. In great contrast, the smaller crystals (Strem and recrystallized) dissolved quickly. The ground Sigma-Aldrich Grubbs' catalyst dissolution is bimodal with two distinct rates of dissolution. Initially there is a high rate of dissolution reflective of the small crystal fragments obtained during grinding. After approximately 10 min the dissolution rate decreases drastically. At this point, the small particles are all completely dissolved and the rate of dissolution is dictated by the larger crystals.

Figure 7 shows the typical healed response of self-healing polymer composites using as-received Strem Chemicals, as-received Sigma-Aldrich, and recrystallized Sigma-Aldrich Grubbs' catalyst that was formed by the addition of a nonsolvent. The self-healing polymer composite system is evaluated by performing fracture tests according to the

- (20) Devotta, I.; Ambekar, V.; Mandhare, A.; Mashelkar, R. *Chem. Eng. Sci.* **1994**, *49* (5), 645–654.
- (21) Peppas, N.; Wu, J.; von Meerwall, E. *Macromolecules* **1994**, *27*, 5626–5638.
- (22) Ghosh, S.; Reed, W. *Biopolymers* **1995**, *35*, 435–450.
- (23) Michel, R.; Reed, W. *Biopolymers* **2000**, *53*, 19–39.
- (24) Parker, A.; Vigouroux, F.; Reed, W. *AIChE J.* **2000**, *46* (7), 1290–1299.
- (25) Raghavan, S.; Ristic, R.; Sheen, D.; Sherwood, J. *J. Pharm. Sci.* **2002**, *91* (10), 2166–2174.

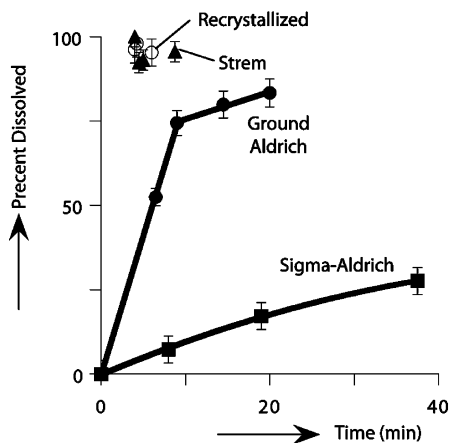


Figure 6. Dissolution rates of various Grubbs' catalyst morphologies.

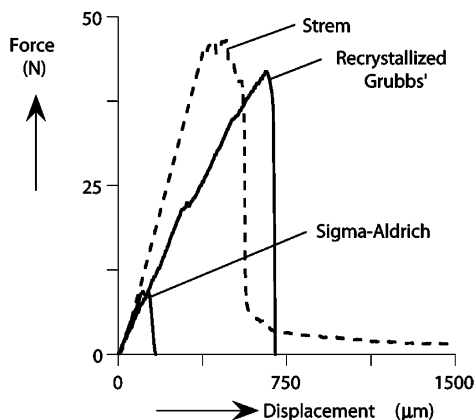


Figure 7. Typical healed response during mode I fracture.

protocol established by Brown et al.<sup>5</sup> In this test a tapered double-cantilever beam specimen is completely fractured under mode I loading. The sample geometry allows the determination of the mode I fracture toughness of the specimen from the elastic modulus, geometrical shape information, and peak load obtained during a fracture test. The maximum load obtained before fracture for the specimen that was healed with Sigma-Aldrich Grubbs' catalyst is 9.2 N, which corresponds to a critical stress intensity for mode I fracture ( $K_{IC}$ ) of 0.11 MPa m<sup>1/2</sup>. Brown et al.<sup>5</sup> found that specimens containing Strem Chemicals Grubbs' catalyst fail at a much higher load of approximately 46.5 N, which corresponds to a  $K_{IC}$  of 0.57 MPa m<sup>1/2</sup>. When the recrystallized catalyst was tested in self-healing specimens, the peak load before fracture of the healed polymer was 41.8 N. As expected, the performance of the nonsolvent recrystallized catalyst is consistent with that of the Strem catalyst.

Unfortunately, the ground Grubbs' catalyst did not provide any better healing capability than the as-received Sigma-Aldrich Grubbs' catalyst (data not shown here). When the catalyst is mixed with the uncured epoxy matrix, it is exposed to the amine curing agent (DETA), which appears to deactivate the catalyst.<sup>26–29</sup> It is presumed that the sub-

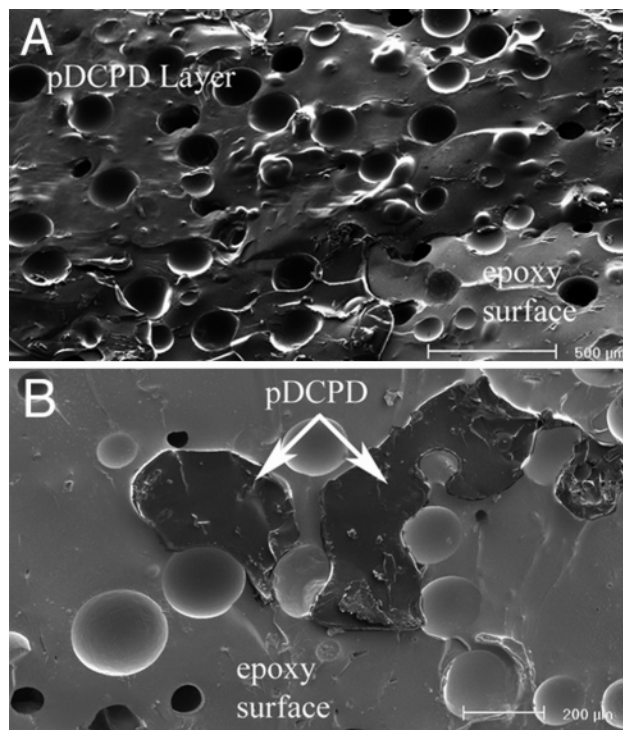


Figure 8. ESEM images of fracture surfaces showing (A) a continuous pDCPD layer from a recrystallized catalyst specimen and (B) partial pDCPD coverage from a Sigma-Aldrich catalyst specimen.

micrometer particles produced during grinding are more susceptible to deactivation during the fabrication of the self-healing polymer composite, and are therefore unreactive with DCPD during the healing stage. Thus, the healing performance depends solely on the remaining larger crystals, resulting in healing efficiencies similar to those of the as-received Sigma-Aldrich Grubbs' catalyst. Similarly, the morphology of the freeze-dried catalyst makes it equally susceptible to deactivation by amine curing agents. The micrometer thick disks (Figure 5C) have fast dissolution kinetics, but need protection during fabrication of the self-healing polymer to prevent deactivation of the catalyst during the fabrication of the polymer composite (details of the protected catalyst system, which is not used in this study, can be found in ref 30).

For high healing efficiency it is desirable that the catalyst dissolves quickly. If the catalyst does not dissolve fast enough, then heterogeneous polymerization occurs in locations where catalyst particles are exposed. Figure 8 shows ESEM images of the fracture planes for two different catalyst morphologies. Figure 8A shows the fracture plane of a self-healing polymer that was fabricated with recrystallized catalyst. This fracture plane has a mostly continuous pDCPD layer. Figure 8B shows the fracture plane of a sample fabricated with as-received Sigma-Aldrich catalyst. Here the polymerization of the healing agent is highly localized near a catalyst particle. With sufficient concentration of catalyst particles exposed on the fracture plane, this partial polymerization will hold the crack closed, but it does not create a continuous pDCPD layer. Thus, the healed sample demon-

(26) Wybrow, R.; Stevenson, N.; Harrity, J. *Synlett* **2004**, 140–142.

(27) Alcaide, B.; Almendros, P.; Alonso, J. *Chem.—Eur. J.* **2003**, *9*, 5793–5799.

(28) Fu, G.; Nguyen, S.; Grubbs, R. *J. Am. Chem. Soc.* **1993**, *115*, 9856–9857.

(29) Wright, D.; Schulte, J.; Page, M. *Org. Lett.* **2000**, *2* (13), 1847–1850.

(30) Rule, J.; Brown, E.; Sottos, N.; White, S.; Moore, J. *Adv. Mater.* **2005**, *17*, 205–208.

strates much lower fracture toughness values. In cases where only a few exposed particles of Grubbs' catalyst are on the fracture plane, there is effectively no healing.

### **Conclusion**

Smaller particles of Grubbs' catalyst dissolve more quickly, leading to a high concentration of catalyst in the healing agent before any significant curing has started, but the fabrication of a self-healing polymer requires the catalyst to survive exposure to amines such as DETA for short periods of time. If the catalyst particles are too small, exposure to the curing agent will significantly reduce the reactivity of the catalyst. By balancing the competing effects of protection during fabrication and fast dissolution in the monomer, self-healing polymers with optimal healing capa-

bilities are produced. We have demonstrated that three crystal morphologies of Grubbs' catalyst are accessible and that they have different dissolution kinetics, thermal stabilities and resistance to deactivation. These properties can be used to tailor the catalyst's properties for specific self-healing applications.

**Acknowledgment.** Financial support from the AFOSR Aerospace and Materials Science Directorate, Mechanics and Materials Program (Grant No. F49620-02-1-0080) is acknowledged. Also, helpful conversations with Terry Craft (Boulder Scientific) about the processing methods of Grubbs' catalyst and the George L. Clark X-Ray Facility and the 3-M Materials Chemistry Lab for assistance with the X-ray diffraction analysis are greatly appreciated.

CM051864S